ANNALS OF GIS
2024, VOL. 30, NO. 4, 455–474
https://doi.org/10.1080/19475683.2024.2380678

Taylor & Francis
Taylor & Francis Group

Arctic accessibility: recent trend in observed ship tracks and validation of arctic transport accessibility model

Weiming Hu[a,b], Guido Cervone[a,c], Luke Trusel[a] and Manzhu Yu[a]

[a]Department of Geography, The Pennsylvania State University, University Park, USA; [b]School of Integrated Sciences, James Madison University, Harrisonburg, USA; [c]Earth and Environmental Systems Institute, The Pennsylvania State University, University Park, USA

ABSTRACT

The Arctic region is undergoing significant changes in maritime accessibility. This study investigates observed ship trajectories from 2013 to 2020 to demonstrate the recent trends of Arctic traffic. A notable surge in maritime activities has been observed, particularly during summer months, driven by economic interests and the increasing popularity of existing routes. Unique patterns in the northern Barents Sea have been observed where ships favour different routes based on seasonal ice conditions. Another contribution from this work is the validation of the Arctic Traffic Accessibility Model (ATAM) using the observed ship traffic data. Results show that the ATAM model underestimates the accessibility and vessel travel speed. This is largely due to outdated model parameters. The predefined ice multipliers and calculation of ice numerals used in the ATAM may not accurately reflect real-world conditions.

ARTICLE HISTORY
Received 8 August 2023
Accepted 8 July 2024

KEYWORDS
Arctic accessibility; maritime traffic; AIS; ATAM; sea ice

1. Introduction

The Arctic plays a critical role in the global environment and ecosystem. The region is experiencing significant impacts from climate change, with temperatures rising at three times the global average, a phenomenon known as the Arctic Amplification (Cohen et al. 2014; Pithan and Mauritsen 2014; Saros et al. 2019; Screen 2014; Serreze and Francis 2006). The impacts of this warming are profound, including permafrost thaw and release of carbon (Turetsky et al. 2020), threats to natural ecosystems and human livelihoods (Hendry et al. 2019), and melting of both land and sea ice at rates that are unprecedented over centuries (Garcia-Soto et al. 2021; Trusel et al. 2018). The decline in the frozen sea ice cover of the Arctic Ocean is one of the most prominent signals of recent Earth system change. Arctic sea ice losses encompass reduced ice extent, age and thickness, with declines occurring in all months but especially pronounced during the annual summer sea ice minimum in September. As a result, all of the lowest ice extents on record have occurred within the last two decades (Meier et al. 2021; Parkinson and DiGirolamo 2021). These changes have far-reaching implications, affecting ecosystems locally and influencing the global climate system by contributing to rising sea levels and extreme events beyond the Arctic.

With the rapidly transforming natural environment comes the potential for new opportunities and access in the Arctic. One signature is the observed increased maritime traffic within and through the Arctic Ocean as the area covered by sea ice has declined in both extent and duration (PAME 2020; Silber and Adams 2019). Data from marine vessel AIS between 2013 and 2019 reveal an overall 25% increase in ships within the Arctic including a 44% increase in vessels transiting the NWP alone (PAME 2020). This accessibility provides the potential for decreased shipping transit times, reduced total emissions and an increasing variety of economic prospects. For example, the Arctic is an area of strategic interest for the United States. Over the last decades, several strategies have been discussed relative to the navigability of the northern routes to increase economic opportunities, military security and tourism (US Department of Defense (2011), White House 2022).

On the other hand, enhanced transit to and through the Arctic raises concerns about the potential damage to the local environment that is already vulnerable (Crépin, Karcher, and Gascard 2017; O'Rourke et al. 2023). For example, the increase in maritime traffic is largely a result of the redistribution of vessels from the southern regions which might introduce non-native plant and animal species (Saebi et al. 2020). The increase in vessel

CONTACT Weiming Hu huwx@jmu.edu School of Integrated Sciences, James Madison University, 800 South Main Street, Harrisonburg, VA 22807, USA
Supplemental data for this article can be accessed online at https://doi.org/10.1080/19475683.2024.2380678.

activities has also coincided with an increase in maritime accidents (Chen et al. 2022). Granier et al. (2006) found that ship traffic through Arctic northern passages could significantly increase surface ozone concentrations, potentially reaching levels comparable to industrialized regions in the Northern Hemisphere. Dalsøren et al. (2012) used climate model projections and showed that shipping emissions in 2030 could increase global and Arctic pollution levels, with the highest impact on ozone during transit season and significant Arctic warming in spring. Researchers have long been aware and concerned about the risks brought forth by the increasing human activities in the Arctic and have been calling out for investments in infrastructure and marine services needed for safe and secure transit with minimal environmental impact (Ho 2010).

Numerous studies in the literature have focused on enhancing and documenting our understanding of the trends and impacts of changes in Arctic maritime traffic. The ATAM (Smith and Stephenson 2013; S. R. Stephenson, Smith, and Agnew 2011) was applied to individual and ensemble-averaged datasets of projected sea ice thickness and concentration from seven different GCM. This was likely the first to quantify the future theoretical increase and opening of new routes at a large scale across the Arctic, following Martin (1988). S. Stephenson and Smith (2015), then, carried out a series of simulations of the Arctic driven by sea ice output from 10 CMIP models and found the choice of climate models significantly impacts Arctic shipping futures, with the eastern Arctic remaining the most accessible marine space for trans-Arctic shipping by mid-century, but the NWP being particularly model-dependent. As a follow-up study on the impact of the redistribution of global shipping traffic, S. Stephenson et al. (2018) found that the trans-Arctic shipping emissions could reduce Arctic warming by nearly 1°C by 2099 due to sulphate-driven liquid water cloud formation. Several parallel studies confirmed the findings that the Arctic sea ice decline will open shorter, and potentially safer and more efficient, trade routes (Aksenov et al. 2017; Marie, Comtois, and Slack 2017; Melia, Haines, and Hawkins 2016). Similarly, Martin Bergström and Kujala (2020) pointed out that decreasing sea ice in the Canadian Arctic had led to significant increases in vessel traffic, with other factors like tourism demand, community re-supply needs and resource exploration also contributing to the increase.

Although many studies have delved into the theoretical relationship between accessibility and changes in the Arctic environment, it would be preferable to observe such a relationship from empirical data. Initially, using the AIS data from 1 January 2015 to 31 December 2017, Silber and Adams (2019) reported no clear trends in the total vessel operations in the Arctic, but inter-year variation is evident with fishing vessels accounting for half of all voyages. However, this could be due to the limited time period. Xiao et al. (2015) carried out detailed comparisons of AIS data analysis between a Dutch case and a Chinese case. Although the study is not particularly focused on the Arctic, it pointed out the challenges in such an analysis due to significant differences in distributions for different characteristics of ship behaviours. Lensu and Goerlandt (2019) produced a database that combines 9 years of AIS data with marine environmental data, enabling the analysis of winter navigation in the Baltic Sea, including close encounters, icebreaker assistance and traffic statistics. The data, although providing critical information by integrating marine environmental data, are application-specific for winter real-time navigation in a limited region. Other challenges of using AIS for traffic analysis and research in the Arctic include the sheer numbers and dimensions of ships (Fiorini, Capata, and Bloisi 2016), scarceness of reporting locations and heterogeneous origins of sensors (2016.

This study aims to validate and improve the current understanding of the trend of Arctic maritime traffic by analysing big spatiotemporal archives of real-time location observations from vessels in the Arctic. We are also interested in how the observed trend from the past decade coincides with the anticipated pattern from theoretical studies in the literature. This study utilizes an 8-year observational dataset of Arctic vessel traffic from 2013 to 2020, together with sea ice and atmospheric reanalysis products, to understand the linkages between observed maritime traffic and sea ice changes.

2. Data

2.1. Study domain

Figure 1 depicts the study's geographic scope, outlining different regions in the Arctic for easy reference throughout the manuscript. The study domain covers major shipping routes such as the NWP, the NSR and the TSR.

2.2. Arctic ship traffic data

AIS is a standard marine data source, primarily used to identify the location of a ship. It uses standard radio waves to broadcast the location, course and other data. The data are routinely collected by shore stations and are generally available worldwide. AIS transmitters are mandatory on almost all ships of a certain size except for

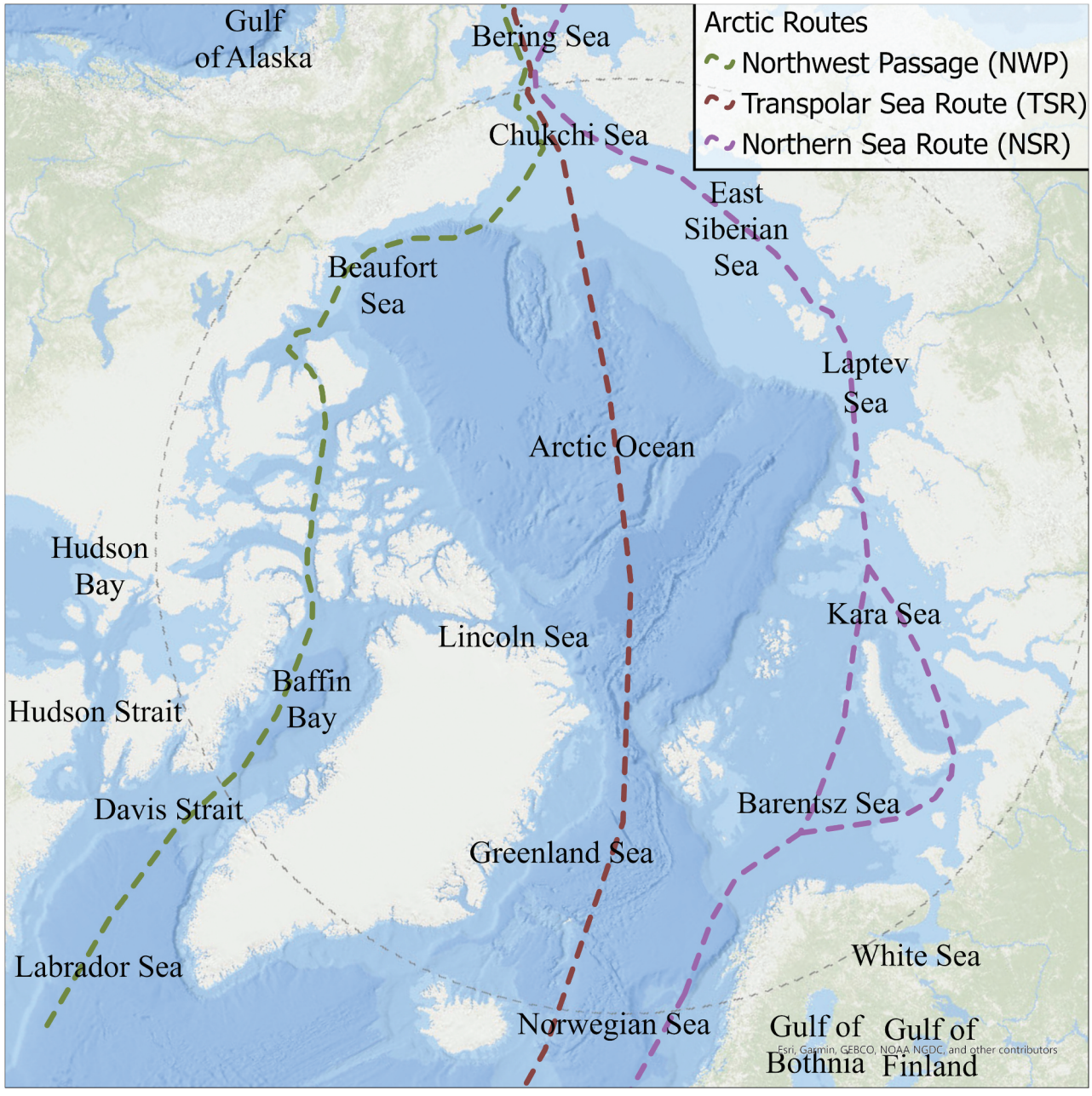

Figure 1. Geographic map of the Arctic region with three major routes across the Arctic.

the military. Continuous AIS data since 2013 for the Arctic region have been compiled under the Arctic Council through the Protection of the Arctic Marine Environment ASTD project. It provides key information on vessel positions, types (e.g. cargo, tanker, passenger, etc.), speeds and other environmental characteristics.

The ASTD and the AIS data both serve as crucial sources of information for monitoring shipping activities in the Arctic region. While both datasets aim to monitor and analyse shipping operations in the Arctic to enhance marine safety and protect the environment, the ASTD system focuses on historical information, including detailed measurements of emissions by ships. The AIS data, on the other hand, provide real-time information on ship positions and movements. In this regard, ASTD aggregates data monthly for each ship, while AIS data provides more immediate and continuous tracking of ship positions. As a result, the ASTD system is utilized by PAME for conducting analysis and developing projects to benefit various working groups.

We collected ASTD (PAME 2020) records from January 2013 to February 2021. This dataset includes emission-related variables including carbon dioxide, sulphur dioxide and black carbon. On average, data are reported

every 6 minutes, but the reporting frequency can be disrupted due to signal loss and device malfunctioning. As a result, although the dataset provides a long period of temporal coverage and high coverage of the shipping activities across the Arctic, these records can be misaligned and intermittent. Another challenge when working with the dataset is how this dataset was originally organized. Data streams were originally saved in one file per month and the unique ship IDs from one file do not remain consistent with the ones saved from the next month. This organization of the data poses difficulties in analysing shipping trajectories that span across multiple months. We are going to introduce, in detail, the data preprocessing procedure in Section 3.1.

2.3. Arctic sea ice volume reanalysis

Sea ice concentration and depth data are collected from the PIOMAS for this study. PIOMAS (Schweiger et al. 2011; Zhang and Andrew Rothrock 2003) is a coupled ocean and sea ice model that simulates daily variables including sea ice concentration, thickness and sea surface temperature. This dataset has been widely validated against other datasets, including ICESat (Kwok et al. 2020; Schweiger et al. 2011; Wang et al. 2016). Uncertainties in sea ice concentration and thickness mostly arise from model forcings, physics and parameterizations. Forcings of wind, thermal and precipitation are typical sources of model uncertainties. A detailed discussion on uncertainties can be found in Schweiger et al. (2011). The dataset covers the period from 1978 to the present. It uses the generalized curvilinear coordinate system centred in Greenland with a spatial coverage from 45°N to 90°N. The resolution is highly variable with an average horizontal resolution of 22 km. To facilitate analysis and visualization of the Arctic region, the PIOMAS has been re-gridded to the Polar Stereographic projection.

3. Methods

This research relies on various techniques to study the spatial patterns of the ship data. Model simulations have also been carried out and verified against the observed records. One of the main challenges is represented by the magnitude of the data, both for the ship tracks which are composed of millions of points (over 500 GB), and for the model simulation output whose analysis itself presents a big challenge. This section discusses the approaches we used to address these challenges.

3.1. ASTD preprocessing procedure

To overcome the challenges mentioned in Section 2.2, we went through rigorous checks and preprocessing steps for the ASTD data before they were used in data visualization and analysis. Figure 2 shows the procedure for preprocessing ASTD records. The original data is stored in CSV files which is not efficient for data analysis. First, records with unknown fields, e.g. an unknown ship category, have been removed to ensure data integrity. Since each record is associated with a unique ship identifier (only within the month), this field is used to filter out rare and abnormal records. For example, any ship identifiers that reported fewer than 10 records are removed because of the relatively low report frequency. We also carried out a visual check on the data to be removed. These records appear to be scattered and discontinued when plotted on a map. Fewer than 1% of the records have been removed after the first two steps, indicating that most of the records are reliable.

A major component in data preprocessing is to create a universal ship identifier across the dataset (spanning multiple months) so that inter-continental shipping trajectories can be correctly analysed and visualized. The merge algorithm is described in the shaded region enclosed by a dotted line in Figure 2. To create a universal ship identifier, the algorithm starts by examining ship ID records from the last day of the leading month and the first day of the subsequent month. The assumption is that shipping trajectories from two consecutive months can only be merged if they have reported records from the last day of the previous month and the first day of the next month. In cases where multiple records exist in this time period, Figure 2 shows the two filtering steps to select the final candidate ship ID for merging. In order for two trajectories to be connected, the ship ID from the subsequent month should (1) have matching attributes with the ship ID from the leading month and (2) have the reported location within a certain distance from the last location from the leading month. The attributes include the vessel category, the PC, the belonging country and the size of the ship. The distance threshold can be calculated based on the reported speed and the direction of the ship. When multiple pairs of trajectories can be found (which can happen when ships are close to ports), the closest pairs are connected. When two trajectories are connected, both trajectories will be assigned the same identifier which is unique throughout the entire dataset.

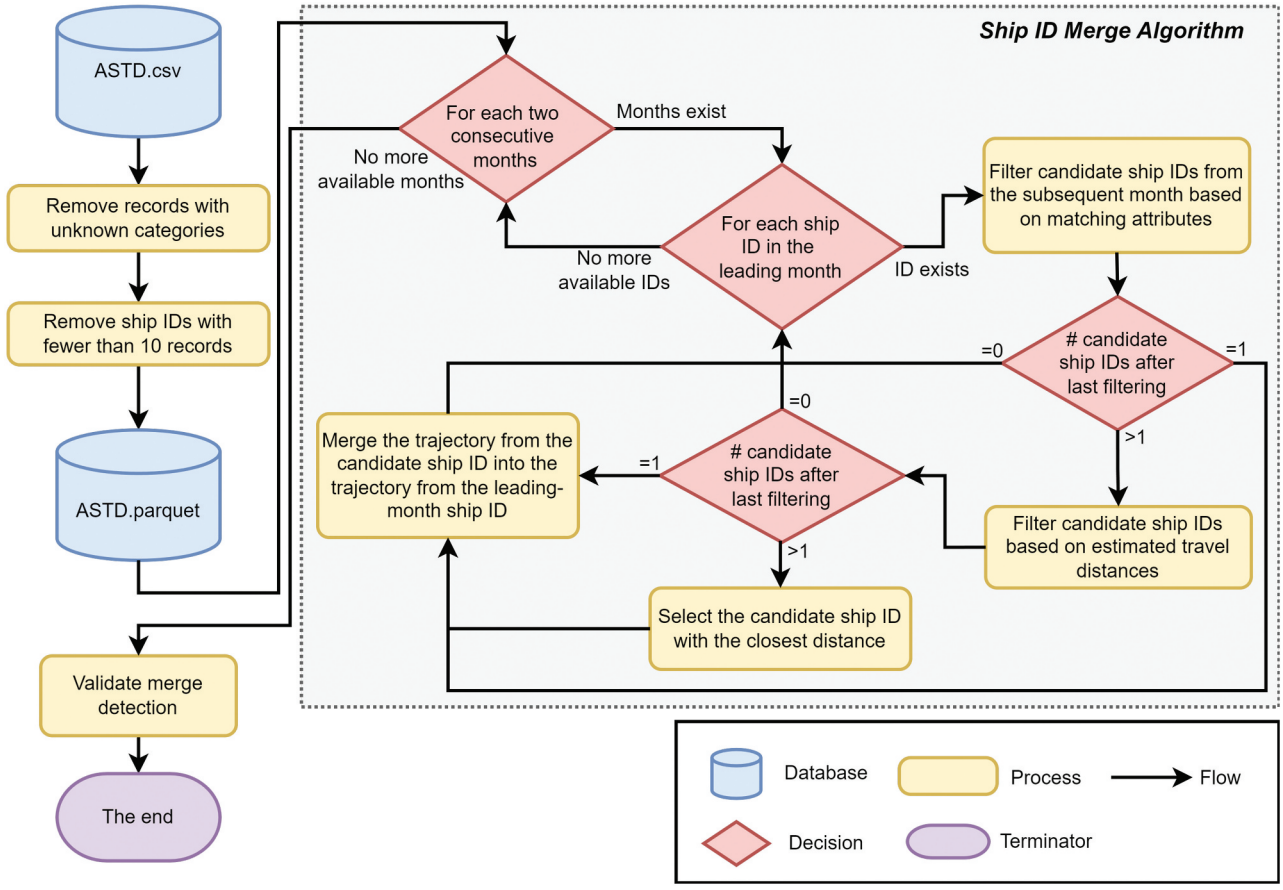

Figure 2. Schematic diagram for data preprocessing.

3.2. Arctic transport accessibility model

The ATAM (Aksenov et al. 2017; Smith and Stephenson 2013; S. R. Stephenson, Smith, and Agnew 2011) is used in this work to study the accessibility and potential transportation routes in the Arctic. Although this framework originally provides both components for modelling land and maritime accessibility and transportation, only the maritime component is used in this study and, therefore, described below.

To quantify the accessibility, ATAM calculates an IN scalar for each grid point. IN indicates the ability of a ship to safely navigate ice-covered water and it is defined as:

$$IN = \sum_{i=1}^{n} C_i M_{i,s}, \tag{1}$$

where C_i is the concentration of ice type i and $M_{i,s}$ is a predefined ice multiplier for ice type i and ship type s. There is not a separate variable that denotes the sea ice age but the multipliers already take this into consideration. They describe the physical properties of ice at the modelled grid point. They are closely related to the ice age because sea ice that has survived more than one summer period referred to as multi-year sea ice, is typically thicker and stronger than younger ice due to the annual accretion of ice layers and reduced brine inclusions. n is the number of simulated ice types depending on the circulation model used. In the case of PIOMAS where only the sea ice concentration and depth are simulated, but not sea ice types, the calculation is simplified to

$$IN = C_{ice} M_{ice,s} + (1 - C_{water}) M_{water,s}. \tag{2}$$

Finally, M is a nonzero integer ranging from −4 to 2. A higher value denotes a lower risk of passing through a particular condition. It is usually predefined based on ice type (i) and ship types (s). However, Smith and Stephenson (2013) provided the mapping functions for two types of vessels, OW (the equivalent of FS II, which stands for open water) and PC6 (the equivalent of FS 1A Super which has ice strengthening), when sea ice depth data are available but not the ice type information:

$$M_{PC6}(t) = \begin{cases} 2, & \text{if } 0 \le t < 0.7 \\ 1, & \text{if } 0.7 \le t < 1.2 \\ -1, & \text{if } 1.2 \le t < 1.51 \\ -3, & \text{if } 1.51 \le t < 1.89 \\ -4, & \text{if } t \ge 1.89, \end{cases} \tag{3}$$

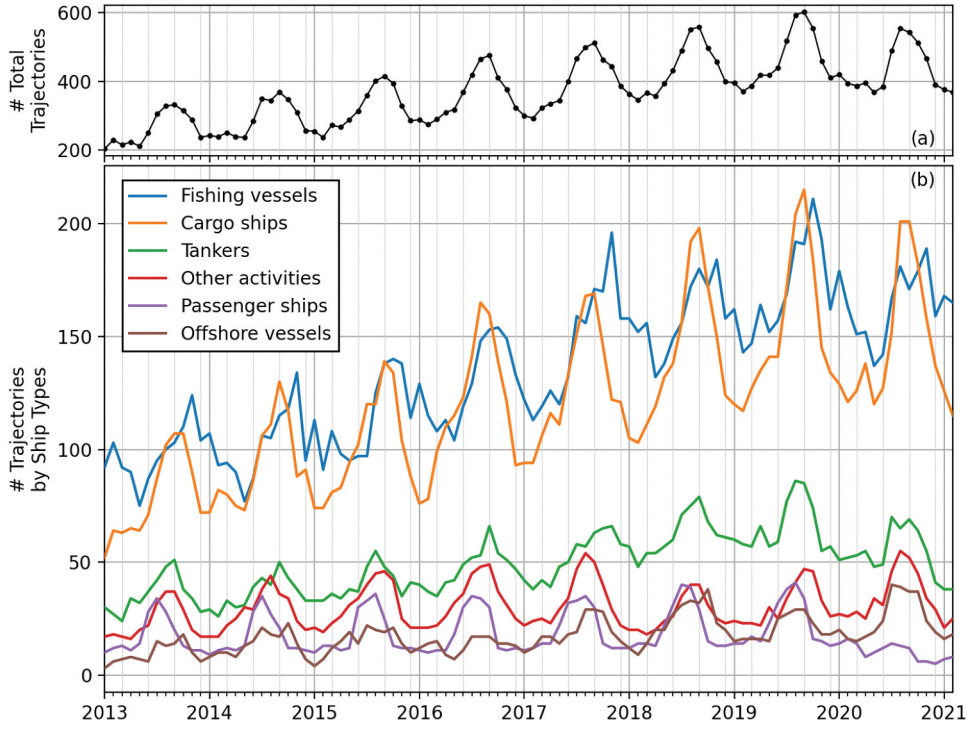

Figure 3. Number of trajectories across the Arctic from 2013 to 2020. (a) shows the total number of trajectories aggregated from all ship types, and (b) shows the numbers of trajectories broken down for each ship type. Each data point represents a monthly sum.

$$M_{OW}(t) = \begin{cases} 2, & \text{if } t = 0 \\ 1, & \text{if } 0 < t < 0.15 \\ -1, & \text{if } 0.15 \leq t < 0.7 \\ -2, & \text{if } 0.7 \leq t < 1.2 \\ -3, & \text{if } 1.2 \leq t < 1.51 \\ -4, & \text{if } t \geq 1.51, \end{cases} \quad (4)$$

where t is the sea ice depth in meters. According to Smith and Stephenson (2013), GCM outputs of ice thickness were categorized into multiplier values by estimating ice type from thickness ranges, using either standard Arctic Ice Regime Shipping System guidelines (for relatively thinner ice) or an empirical regression model based on analysis of remotely sensed data (for thicker ice, $>$ 120 cm). The bins of sea ice thickness are defined as such to differentiate types of sea ice, including multi-year, second-year and first-year ice. There is no −2 for PC6 which might be the result of the regression model and a rounding number.

The steps to calculate IN at a particular grid point are described as follows: first, the sea ice concentration and depth are retrieved from PIOMAS; then, the ice multiplier can be calculated given a ship type (s) and the sea ice depth (t); finally, IN can be calculated based on Equation 2. $M_{water,s}$ can be calculated as $M_s(0)$. This process is then repeated at all grid points to calculate IN for the entire domain.

Maritime navigation and transportation can then refer to IN, as a higher IN denotes a safer condition and better accessibility. A negative IN denotes that the grid point is inaccessible for the particular ship type. The ice numeral maps, therefore, can serve as theoretical accessibility maps that can then be compared with the observed ship locations. Furthermore, average safe speed in knots can be derived as a function of IN. In this work, we used the look-up table, the supplementary Table 5, from S. R. Stephenson, Smith, and Agnew (2011) to convert IN to travel speeds.

4. Results

4.1. Recent trends in arctic ship trajectories

Figure 3 characterizes the temporal trend of the number of trajectories across the Arctic from 2013 to 2020. Figure 3a shows the total number of trajectories for all ship types and Figure 3b shows the trajectory counts broken down for each ship type. The total number of trajectories has seen a steady increase from 2013, almost doubling in September when the Arctic sea ice extent is usually at its annual lowest. The increasing trend is not only visible in summers but also in winters when crossing the Arctic is typically advised against due to unfavourable maritime conditions.

Figure 3b further shows how the change from each type of ship contributes to the overall variation. The two main driving factors for the grand total increase are

fishing vessels and cargo ships. Cargo ships contain several subtypes including bulk carriers, container ships, general cargo ships, refrigerated cargo ships and roll-on-roll-off cargo ships. These ships are extremely adaptable and can be used to transport a wide array of goods including either containerized merchants or unpackaged goods like grain or coal. Fishing vessels are also on the rise with the climax appearing in late summers and early winters. The third major impact comes from tankers that carry liquid cargoes in bulk and are responsible for transporting most of the world's energy needs, including crude oil, refined petroleum, gas and chemicals. Its year-round pattern resembles that of cargo ships.

Figure 4 presents similar results on the total number of trajectories but specifically along the NWP and NSR. Aside from the increasing pattern, the total number of trajectories along the NWP was significantly impacted in 2020 due to a reduction of passenger ships which has historically shown dominance in the total count that amounts to 40% (Figure 4a). The numbers of cargo ships and tankers were not impacted during this time. On the other hand, in Figure 4c, trajectories along NSR were historically dominated by cargo ships and tankers which account for over 95% of the traffic. Figure 4(b,d) show the composition of traffic by FS ice class. Ice-strengthened ships are highly common along both routes due to difficult ice conditions in these regions.

Figure 5 shows maps of the Arctic maritime traffic coloured by the most frequently visiting counties (a) and by the number of counties that visited at least once (b) from 2013 to 2020. As shown in Figure 5a, generally, Russian vessels dominate the NSR with most of the activities being fishing and commercial shipping. On the contrary, the NWP has been traversed by a number of countries including Denmark, Panama and Canada as the most frequent visitors.

In terms of the diversity of countries in the Arctic, as shown in Figure 5b, the most diverse regions are the Norwegian Sea and the Barents Sea. From 2013 to 2020, more than 50 countries worldwide have sent ships across these regions, mostly following the coastline of northern Norway and heading towards the Port of Murmansk, Russia. Figure A1 provides a zoomed-in view of the selected trajectories that are particularly close to the North Pole.

To demonstrate the increasing traffic and accessibility in different regions of the Arctic, Figure 6 summarizes the total number of trajectories by years and months for four regions of the Arctic, the NWP, the eastern Kara Sea and the northern and southern Barents Sea. Ship trajectories crossing these four regions have been grouped and aggregated to calculate a monthly summary. The NWP is accessible during summers, but the accessible window has been consistent. In 2013, fewer than 20 ship

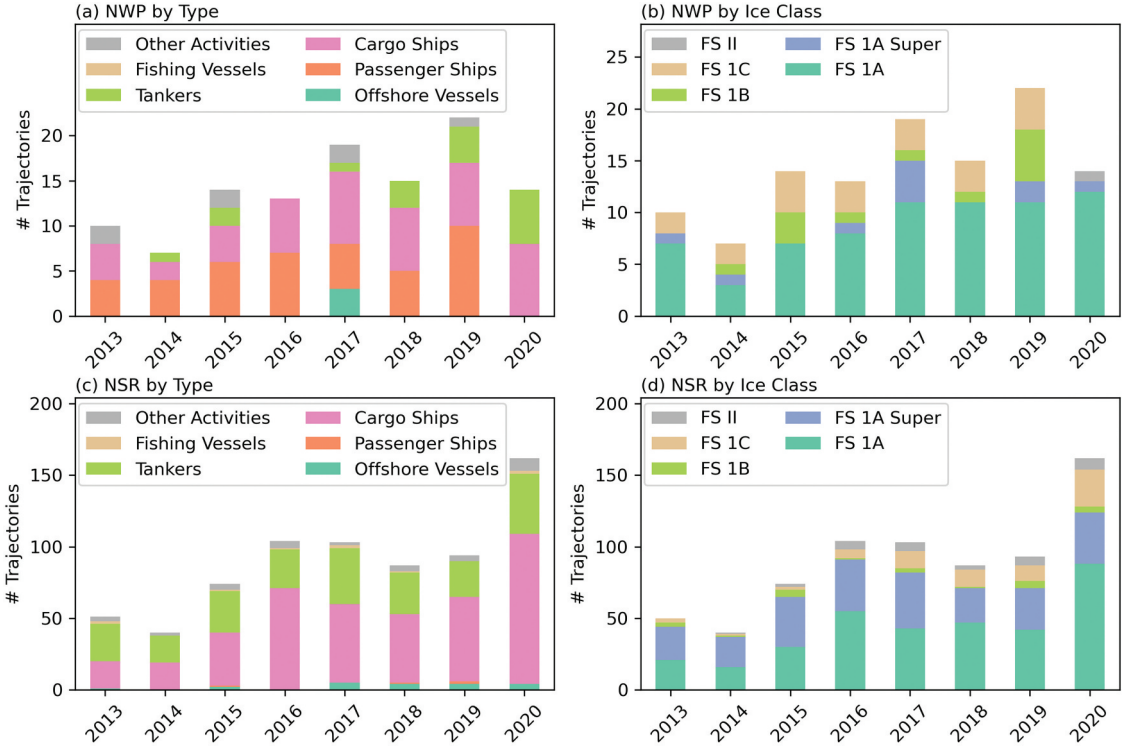

Figure 4. Total number of trajectories across years as categorized by the ship types and ice strengthening class (FS). (a, b) are generated with trajectories along NWP; (c, d) are generated with trajectories along NSR.

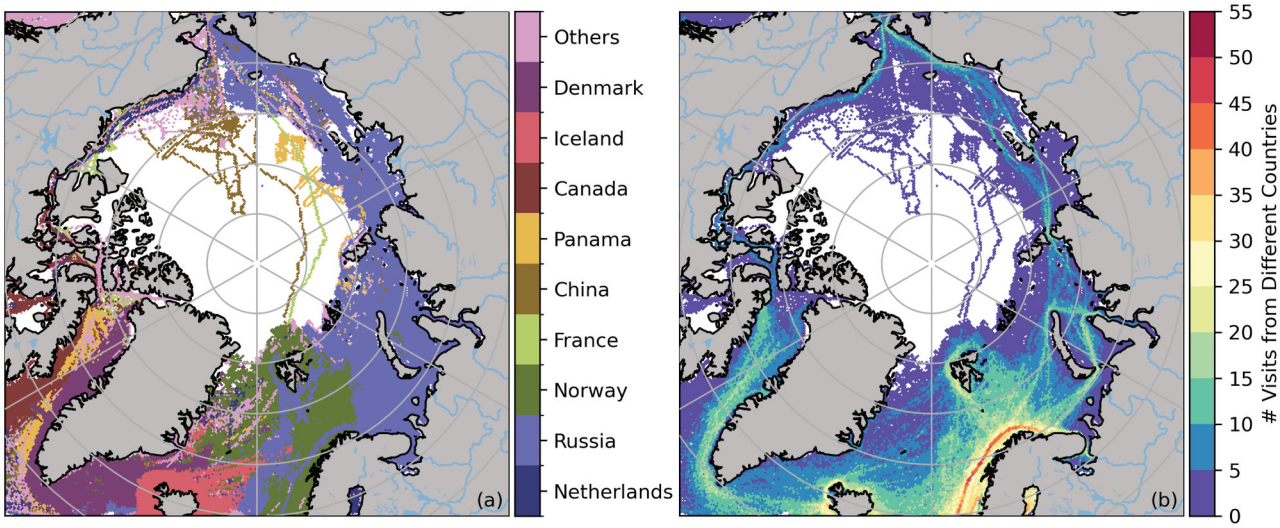

Figure 5. Geographic maps of the Arctic with colors corresponding to (a) the country that visited the particular grid most frequently between 2013 and 2020 and (b) the number of countries that at least visited a particular grid once between 2013 and 2020.

trajectories traversed the NWP, most of which clustered in late August and early September. Since then, the number of trajectories has been on the rise until 2019, reaching over 50 trajectories during August. The bottom panel shows the decomposition of ship types associated with the trajectories. Around 80% of the ships passing the NWP belong to the FS I which is only strengthened for thin ice.

Figure 6(5–8) shows the accessibility change over the eastern Arctic region. In general, this water has been more frequently visited compared to the NWP. The eastern Kara Sea and the southern Barents Sea share a similar trend: an increasing number of ships have passed these regions and the accessible time frame has increased from initially barely over a month to recently well over 3 months.

The trend in the northern Barents Sea is unique. The northern Barents Sea has shown a similar accessibility level throughout the year since 2015. In 2016, 2017 and 2019, the number of trajectories during late winters and early springs makes up for the most part of the annual total, while summers are usually the most accessible time for the other seas. By comparing the FS ice classes, FS I ships (strengthened for thin ice) make up the majority of ships in the other regions. In contrast, the dominating ship type in the northern Barents Sea changes from FS 1A Super in springs to FS I in summers. This shift will be discussed more in detail in Section 5.2.

4.2. Navigational conditions in the Arctic

To further understand how navigational conditions impact Arctic accessibility, this section presents results on maritime traffic from the analysis encompassing both sea ice dynamics and traffic patterns.

The ship trajectories in Figure A1 present a great opportunity to observe the relationship between navigational conditions and accessibility as these ships first travel through open waters and then through ice-infested regions, allowing us to analyse the change in travel speed as a function of navigational conditions. Figure 7 shows a case study with data from the Chinese visit from 2018/08/04 to 2018/09/16. The vessel had an ice class of FS 1A and was marked as other activities. It entered the Arctic Ocean from the Beaufort Sea while approaching the North Pole. The northmost location was reported around 85°N before the vessel returned. Figures 7(a,b) show the travel speed and sea ice conditions (concentration and depth) as a function of time. Figure 7c shows the negatively correlated relationship between sea ice depth and travel speed with a correlation coefficient of −0.83.

Figure 8 shows the aggregated results from various ship types and ice classes. With the increasing depth of surrounding sea ice, the travel speed decreases. However, its variation is related to the ship type and ice class. The FS II vessels (last column) are limited in terms of traversing ice-infested regions by design but exceptions do exist for cargo, fishing and passenger ships. Horizontally, we can observe the role of ice strengthening for a specific ship type. Generally, moving from left to right (stronger to weaker hulls), the right tail becomes shorter meaning that ships would be less likely to visit in ice-infested regions. Pearson correlation coefficients between sea ice depth and travel speed have been calculated for all combinations of ship types and ice classes. The relationship and exceptions will be further discussed in Section 5.3.

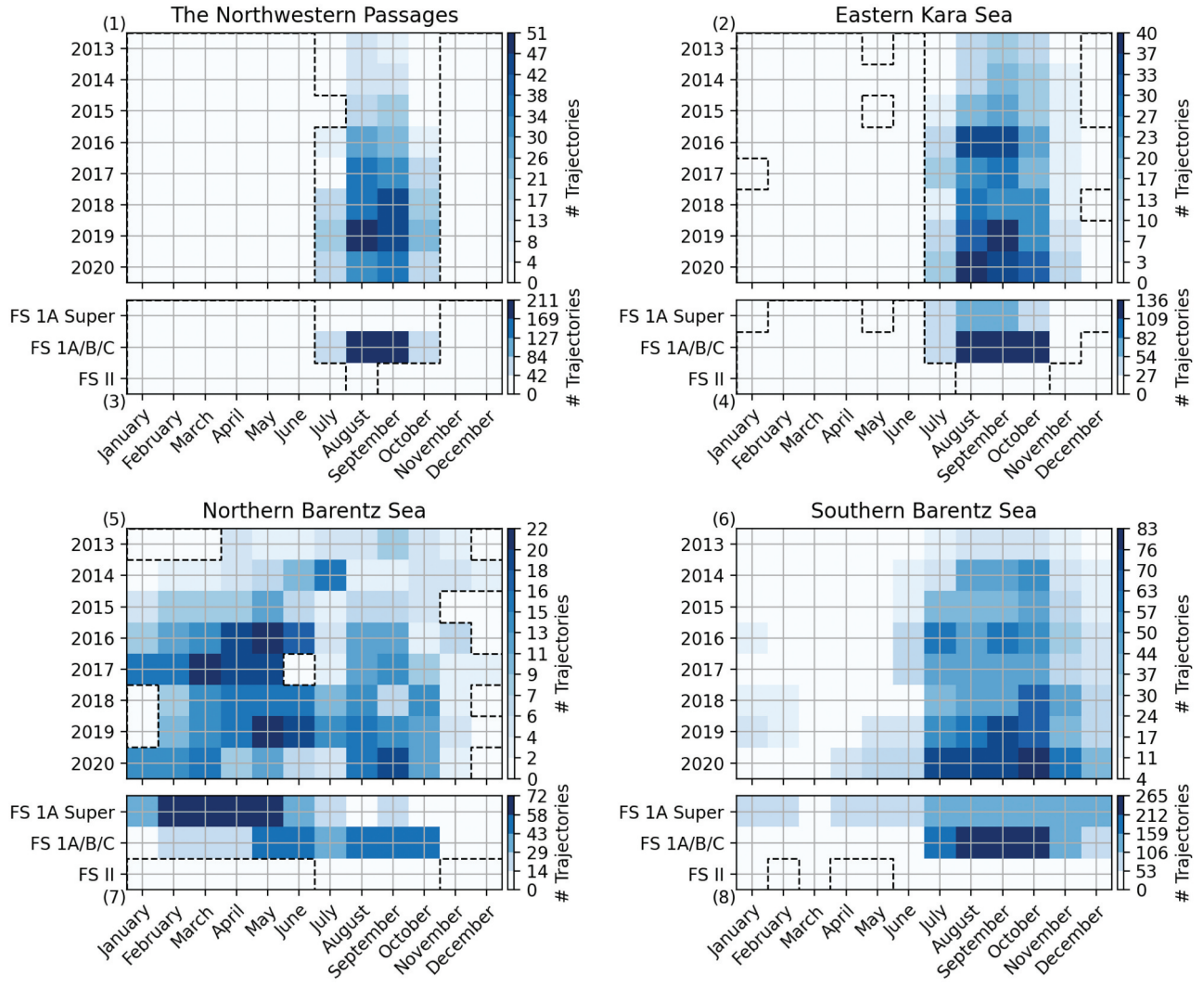

Figure 6. Heat maps of numbers of trajectories recorded within four regions, the northwestern passages (1, 3), eastern Kara Sea (2, 4), northern Barents Sea (5, 7) and southern Barents Sea (6, 8) within the Arctic region. Dashed black lines separate blocks having zero trajectories and at least one trajectory.

Zooming to a larger scale, Figure 9 compares the sea ice concentration with the frequency of observed ship visits. The sea ice concentration is calculated as a monthly median and the number of ship visits on each grid is defined as the number of unique trajectories passing the specific grid during the 1-month period. Sea ice concentration is an important indicator for maritime navigation, and hence, there is a strong negative correlation between the locations of sea ice and observed ship visits. Overall, fewer ships navigate through the NWP than the other three regions on the east. Trajectories into the NWP typically stop at ports on the western coast of Greenland during winters and springs, and no trajectories are crossing the NWP until summers. Even during September, most ships present in the NWP typically only visit Baffin Bay without navigating deep into the Canadian Arctic Archipelago.

4.3. Validation of arctic transport accessibility model

In the previous section, the ASTD dataset is compared with PIOMAS and it has been shown that the sea ice extent plays a fundamental role in the navigation of shipping activities. To better evaluate how well these two phenomena are related, we rely on the comparison between the ASTD and model simulations from the ATAM.

First, the comparison between model simulation and ship observations is carried out in space. Figure 10 shows the sea ice conditions retrieved from PIOMAS and the calculated ice numerals from ATAM for two types of ships: PC6 (the equivalent of FS 1A Super) and OW (the equivalent of FS II, which stands for open water). Ice numeral provides a measure for accessibility: a higher

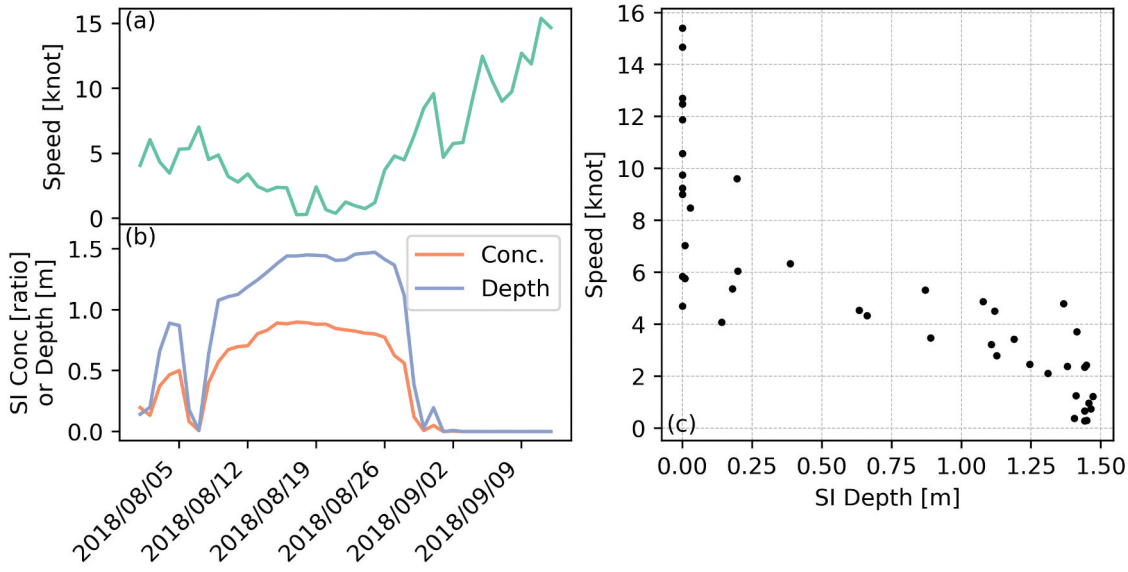

Figure 7. A case study of the Chinese ship trajectory from 2018/08/04 to 2018/09/16 shown in figure A1. (a) shows the daily average travel speed; (b) shows the average sea ice concentration and depth over the traversed region during a particular day; (c) shows the speed of the ship as a function of sea ice depth. Note that sea ice concentration is a ratio from 0 to 1 while depth is a non-negative scalar.

positive number is associated with a faster travel speed and a negative number indicates the area is inaccessible. The monthly medians of sea ice concentration and thickness are calculated and shown for each grid. PC6 ships are strengthened to navigate through difficult ice-infested waters, and therefore, during February, the southern Baffin Bay and the northern Kara Sea are accessible for PC6 ships, indicated by the green regions in Figure 10c, even though waters are still covered in sea ice. PC6 ships are therefore capable of travelling from the northern Barents Sea to minimize the distance and the risk of travelling on ice.

Different from PC6 ships, OW ships should be operated further away from any sea ice due to their thinner hull. No trajectories were observed during the same period in southern Baffin Bay. A few trajectories were observed in the Greenland Sea, the Norwegian Sea and the Barents Sea close to coastlines. These trajectories are mostly fishing and cargo ships. ATAM simulation correctly determines these regions as accessible, instead of marking the Kara Sea as inaccessible for OW ships.

Figure 11 and Figure 12 show similar maps but for June and September. The NWP remains inaccessible for both types in June while the Kara Sea has already opened up for PC6 ships and most of the ships are travelling from the southern Barents Sea. During Summer 2019 when the Arctic ice extent reaches its annual minimum, the NSR sees an increase in traffic, especially in inter-continental shipping.

To better understand when the accessibility of the Arctic can be better modelled, Figure 13 shows the rose diagrams for a number of metrics characterizing the temporal trend of the Arctic accessibility and the simulation accuracy. The metrics were first calculated across all grid points for each month and each year from 2013 to 2020, and then they were grouped to produce monthly maximums, medians and minimums. Figure 13(a,b) demonstrates the total area where the ATAM has simulated as inaccessible but ships have been observed from ASTD, as referred to as the false-negative region. The missed area for PC6 ships peaks around May but it remains low for the remainder of the year. The temporal trend of the missed area for OW ships, shown in Figure 13b, reveals a similar situation. The earliest time for OW ships to safely travel through the Arctic can range from June to August. The absolute values of missed area for OW ships are also smaller than those for PC6 ships. Note the missed area is close to zero during winters, but this could be related to the fact the Arctic is largely inaccessible for OW ships during winter and to the lack of observations.

Figure 13(c,d,e) shows the ice covered area and the observed area for PC6 and OW ships. While there are ships observed year-round in the Arctic, ships observed during February and March can be located at lower latitudes where open water is perennial. PC6 and OW ships have the largest differences in their observed area in December and May, and PC6 ships are less impacted by the annual variation of sea ice due to the higher level of ice strengthening.

Figure 13 only shows the temporal tendency of which months are more likely to be misrepresented by the ATAM in terms of accessibility. In addition, we carried out a similar analysis but in space, as shown in Figure 14, to illustrate the spatial distribution of where the missed

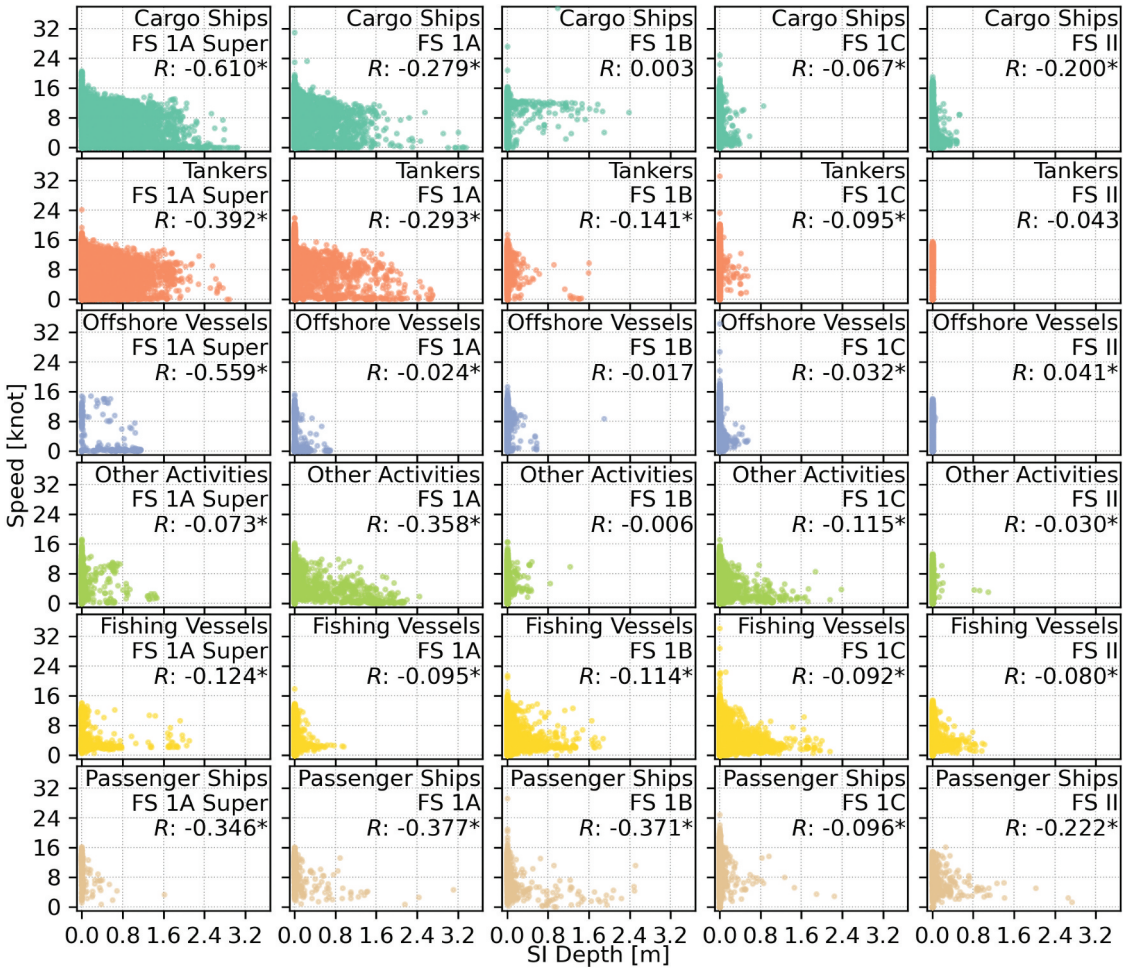

Figure 8. Vessel travel speed as a function of sea ice depth. Panels are organized by their ship types (the first label on the upper right) by rows and ice classes (the second label on the upper right) by columns. Pearson correlation coefficient (*R*) is shown. An asterisk is appended if it is significantly different from zero with a 95% confidence interval estimated by bootstrapping.

locations can be. Each grid is colour-coded based on the number of total days when the grid is determined as inaccessible by ATAM but ships have been observed in the ASTD. The misrepresented area for PC6 clusters around the Kara Sea, specifically around the northern Kara Sea. This suggests that the ATAM simulation can be too conservative at allowing ice-strengthening ships to travel into the sea ice. OW ships see a lower number of missed grids as being accessible. The missed area largely clustered to the north of Svalbard. Previously, Figure 9(6) shows that a small portion of OW ships can travel close to where sea ice is shown to be. These ships could be escorted by ice breakers or there might be the uncertainty of the exact extent of sea ice from the PIOMAS dataset which drives ATAM simulations.

Finally, Figure 15 the observed and the estimated travel speed. Since the travel speed is a function of both sea ice concentration (to calculate the ratio of open water and sea ice) and depth (to calculate the ice multiplier), the travel speed is shown in colours. For PC6, ATAM is significantly underestimating the travel speed. The lookup table from S. R. Stephenson, Smith, and Agnew (2011) was originally developed by McCallum et al. (1996). Technological advancements over the past few decades may render this table outdated. In fact, for PC6 ships, the highest possible speed from ATAM calculation is four knots which is already significantly below the observed travel speed. Another major discrepancy between Figure 15(a,b) is that the observed speed map has a higher variation while the estimated map has a bifurcation when the sea ice depth increases beyond about 1.2 m. This is largely due to the wide bins in Equation 3 for sea ice depth. On the other hand, ATAM is shown to better represent the average speed of OW ships although it underestimates in open waters and over-estimates in regions with first-year ice. The lack of variability in the speed estimation still persists.

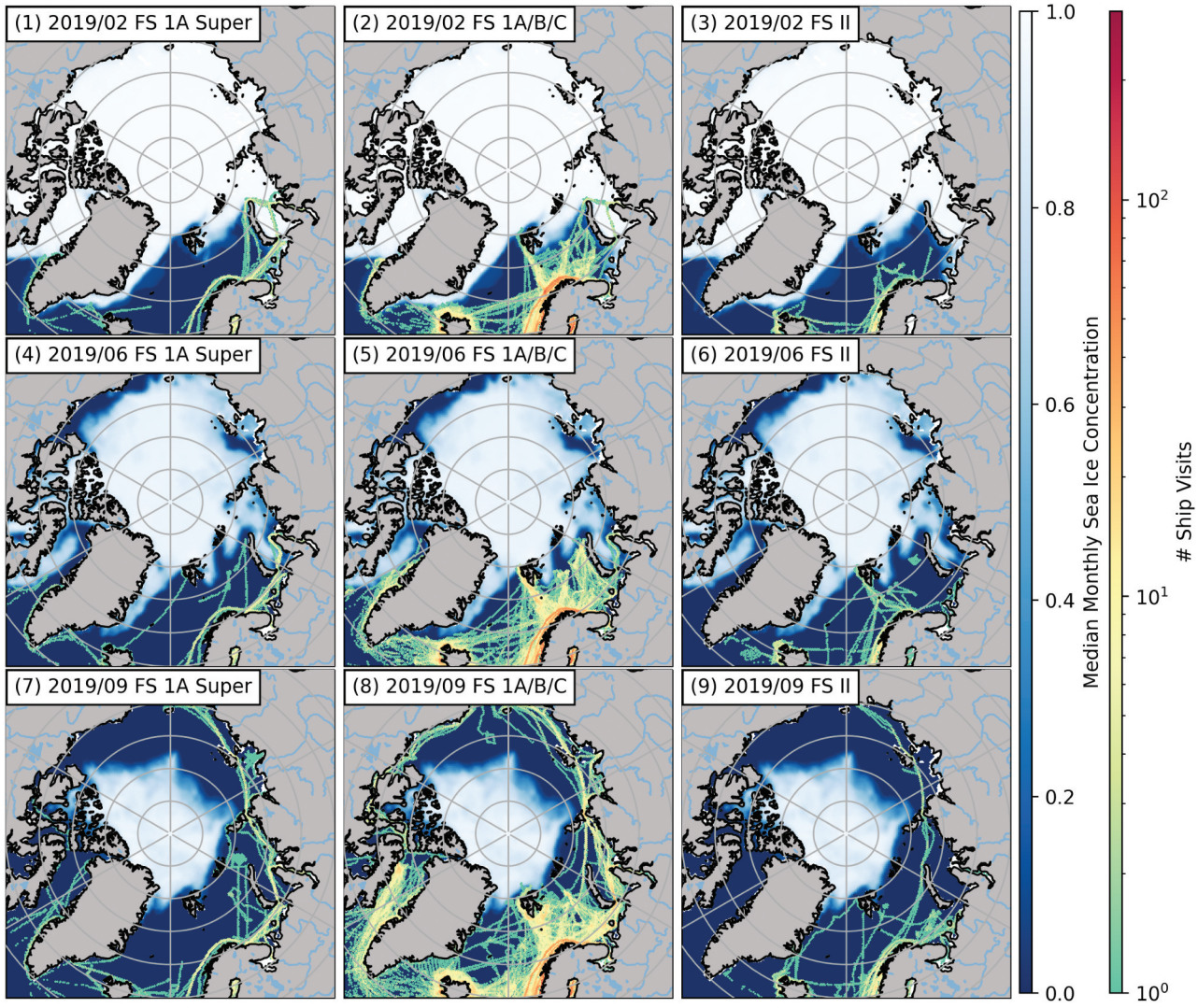

Figure 9. Geographic maps of the Arctic with the base layer corresponding to the ice concentration and the top layer corresponding to the spatial distribution of observed ship visits. The color of the points shows the frequency of observed ship visits on a logarithmic scale.

5. Discussion

5.1. Major factors in Arctic traffic

The examination of ship trajectories from 2013 to 2020, from Figures 3 and 4, reveals a notable increase in maritime traffic across the Arctic. This trend is particularly pronounced during the summer months, traditionally characterized by reduced sea ice extent. The increase in ship activities, even during winter months, underscores the changing accessibility of Arctic waters, facilitated by diminishing sea ice cover and improving navigational capabilities. Fishing vessels and cargo ships emerge as key drivers of this upward trajectory, reflecting both economic interests and the increasing popularity of existing maritime routes.

The negative impact of COVID-19 can be observed in all ship types indicated by either the staggering or decreasing numbers of total trajectories in 2020. This impact can be best observed from passenger ships whose activities are closely related to tourism. Springs and summers are popular seasons for visiting the Arctic region, but this tradition came to a sudden halt in 2020 due to the outbreak of the pandemic and the strict travel regulations in place. Annual tanker activities shift to a downward trend starting in 2020 mostly due to the reduced global oil demand and the disruption in supply chains.

Zooming into the two major routes across the Arctic. In general, NSR received more ship visits than NWP. Aside from the apparent difficulties of navigating through the complex geography, another reason is that most of the ships in NWP belong to FS I which has only minimal ice strengthening and they typically need assistance from an icebreaker when travelling through ice-infested areas.

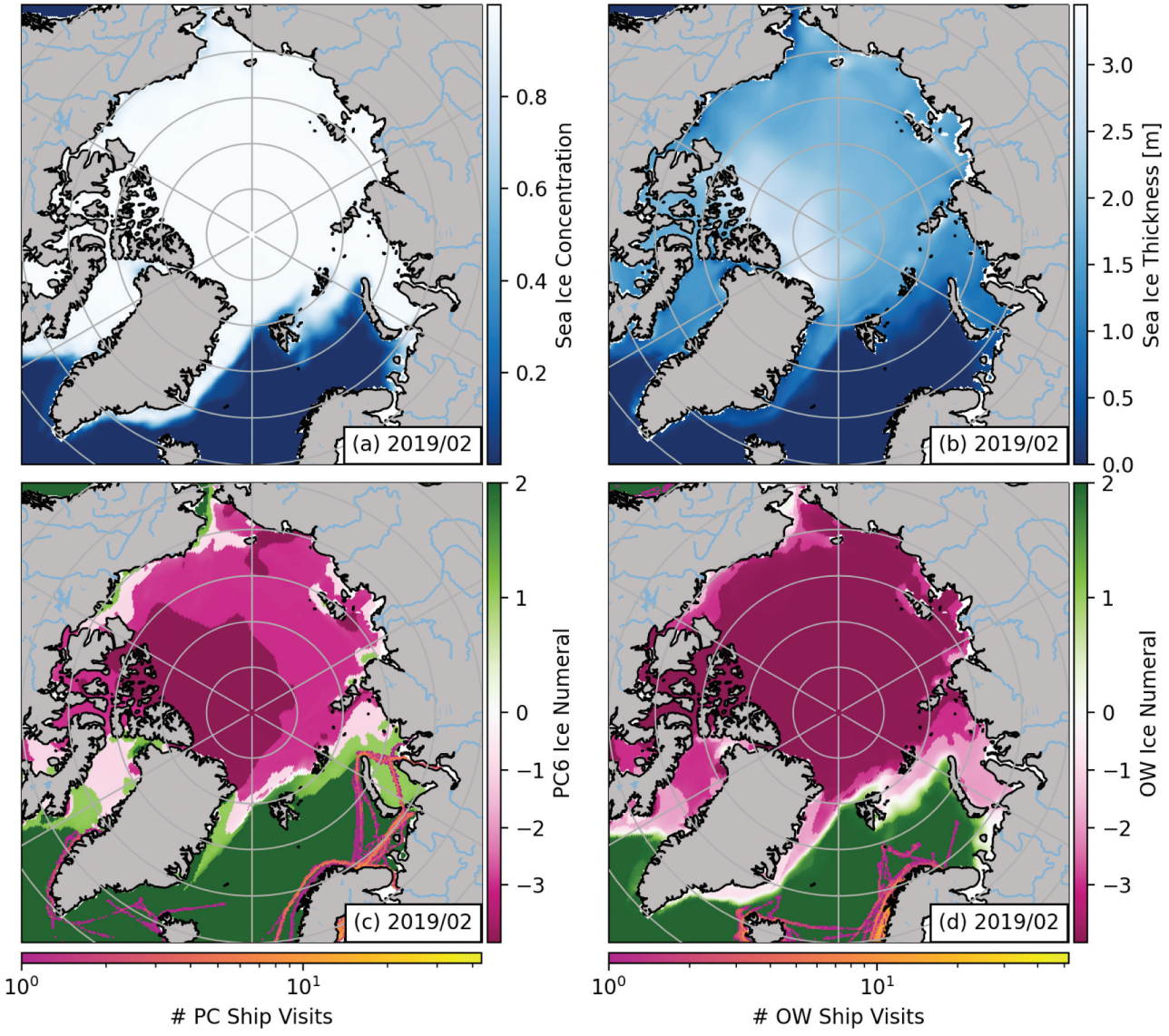

Figure 10. Geographic maps of the Arctic with (a) monthly median of sea ice concentration, (b) sea ice thickness and ice numerals calculated for (c) PC6 and (d) OW ships. Observed ship locations are shown as points on (c) and (d) with their colors corresponding to visit frequency. The aggregation period is 2019 February.

Figures 4(a,c) show that the ship trajectories along NWP decreased in 2020 due to the loss of passenger ships. However, all the other types have remained at a similar level or even seen an increase, as in the case of NSR. The resilience of cargo shipping, even amidst global disruptions like the COVID-19 pandemic, highlights the strategic importance of Arctic routes for international trade.

The great diversity of nations (Figure 5) of NWP also suggests strong international interest in accessing the resources and navigable waters along Norway and northwest Russia's coasts. Comparing the Barents Sea, however, the NWP has far more challenges in terms of navigation and accessibility due to its prolonged period of sea ice cover and shallow, complex waterways. As a result, only a few countries (< 5) have ever set sail to this route.

5.2. Unique pattern in northern Barents Sea

The accessible window in the Arctic refers to the period during which maritime navigation is feasible due to reduced sea ice cover or observation. This window is undergoing significant changes, as evidenced by the findings of this study. Over the past decade, there has been a notable increase in the duration of this accessible window and the frequency of visits. This can be observed in NWP, eastern Kara Sea and southern Barents Sea, based on their reversed funnel shape in Figure 6 which indicates that more ships are visiting the region and the window of accessibility is becoming longer.

However, Figure 6(5) shows a unique trend for the northern Barents Sea. During summer when sea

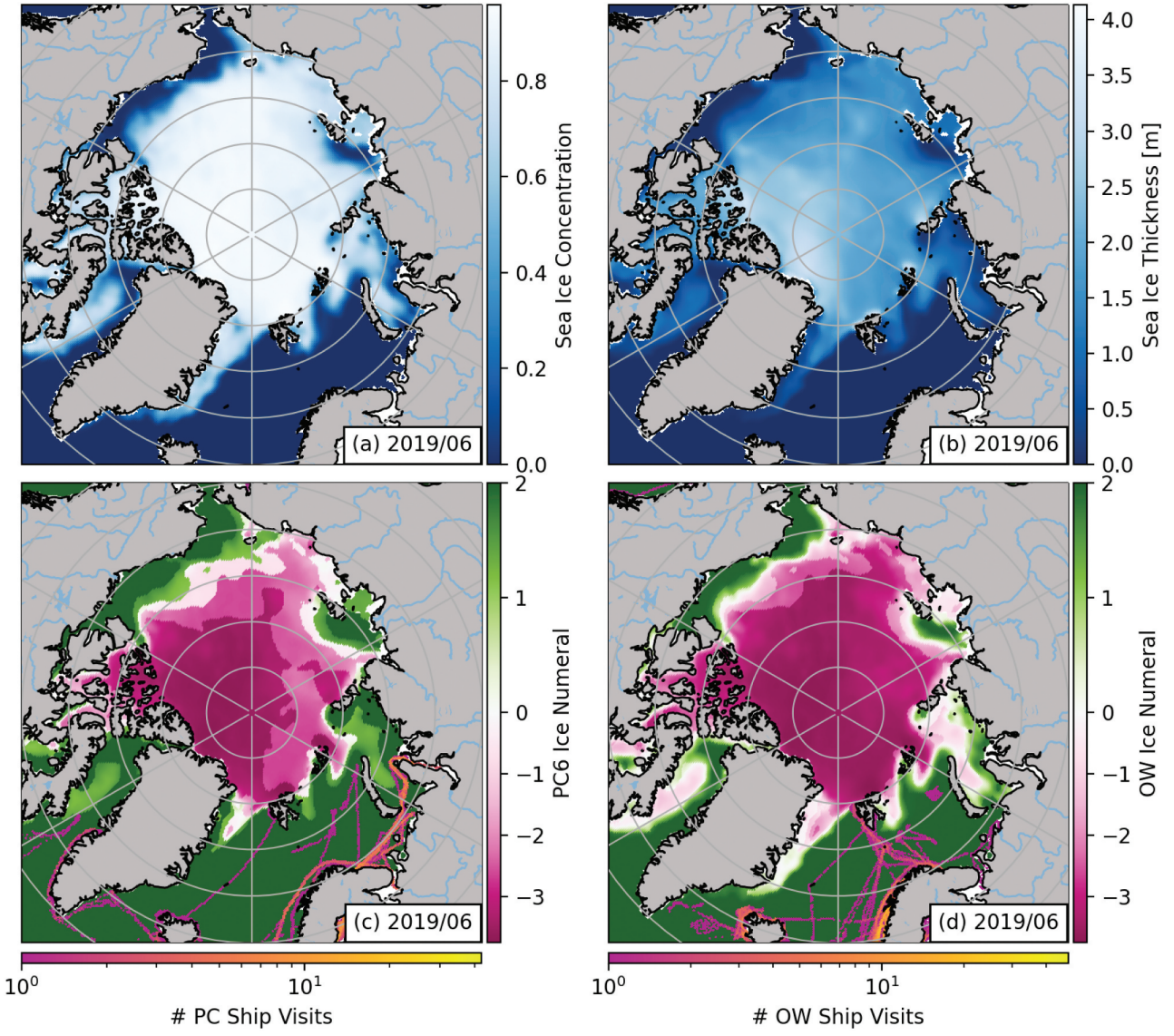

Figure 11. Geographic maps of the Arctic with (a) monthly median of sea ice concentration, (b) sea ice thickness and ice numerals calculated for (c) PC6 and (d) OW ships. Observed ship locations are shown as points on (c) and (d) with their colors corresponding to visit frequency. The aggregation period is 2019 June.

ice melting is at its peak, ships prefer to pass through the southern Barents Sea. However, in spring, this route is heavily ice-infested and not accessible. As a result, ships generally re-route to the northern Barents Sea and adopt a slightly shorter path on ice with a higher FS class to operate in difficult ice conditions.

Figure 9(1,2) further illustrates the reason for the reversed trend observed in the northern Barents Sea. During winters, the Kara Sea is covered in sea ice and largely inaccessible. Ships travelling from the Barents Sea to the Kara Sea require assistance from ice breakers no matter which route they choose, but, if going through the northern Barents Sea, they can minimize travel time on ice (shorter path). Therefore, the northern Barents Sea becomes a favourable route during this time. As the temperature rises and sea ice starts to melt in springs and early summers, as shown in Figures 9(4,5), ships start to switch back to the southern Barents Sea which is less covered in ice to minimize navigational risks. The number of FS 1A super ships also decreases due to a drop in demand. During late summers, as shown in Figures 9(7–9), the Sannikov Strait on the eastern Kara Sea opens up. This allows ships to travel along the NSR and the northern Barents Sea hence having more traffic due to the increase of intercontinental shipping activities.

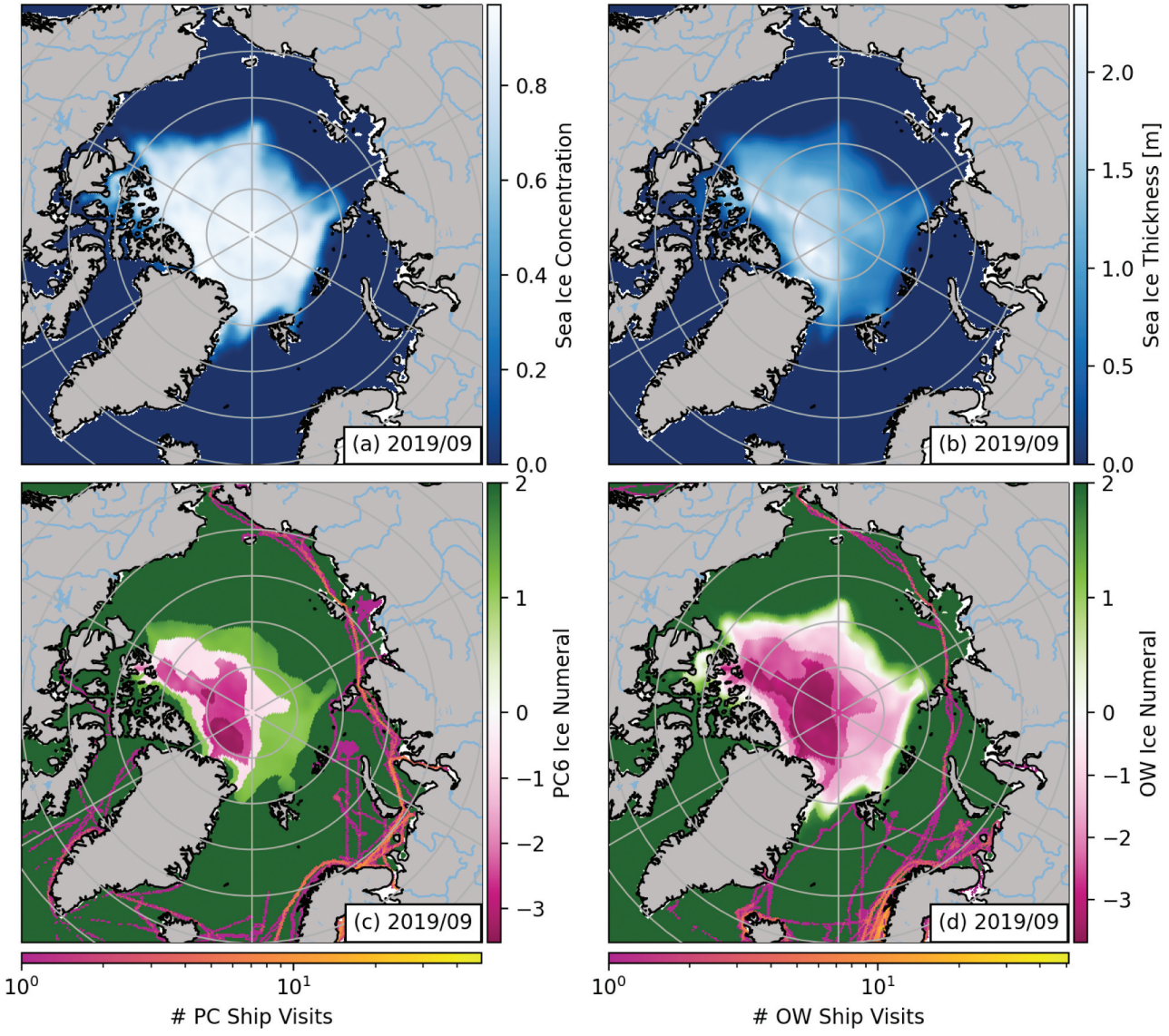

Figure 12. Geographic maps of the Arctic with (a) monthly median of sea ice concentration, (b) sea ice thickness and ice numerals calculated for (c) PC6 and (d) OW ships. Observed ship locations are shown as points on (c) and (d) with their colors corresponding to visit frequency. The aggregation period is 2019 September.

5.3. Relationship between navigational conditions and ship visits

The analysis of navigational conditions sheds light on the relationship between sea ice dynamics and ship accessibility. The observed inverse correlation between travel speed and sea ice depth underscores the impact of ice conditions on maritime operations. Ice-strengthened vessels, particularly those with FS 1A Super classification, demonstrate higher capability in navigating through ice-infested regions, while ships with thinner hulls exhibit reduced flexibility and rely on safer, open-water routes.

In Figure 8, vessels like cargo ships and tankers usually carry a large volume of goods and travel long distances. To minimize risks and costs, their travel speed varies closely with the change in sea ice conditions. Offshore vessels are similar but they typically do not enter the deep Arctic Ocean (observed by having shorter tails in scatter plots) because they usually have operational purposes including oil exploration, construction work or providing supplies on the high seas. However, fishing vessels do not show the same amount of decline when the FS class moves down. Fishing vessels are shown to visit regions covered by first-year ice (sea ice depth smaller than 1.5 metres). This could be due to the resource richness. Some ice-infested regions can be abundant in marine life, including fish species such as cod, haddock and halibut. Fishing vessels may venture

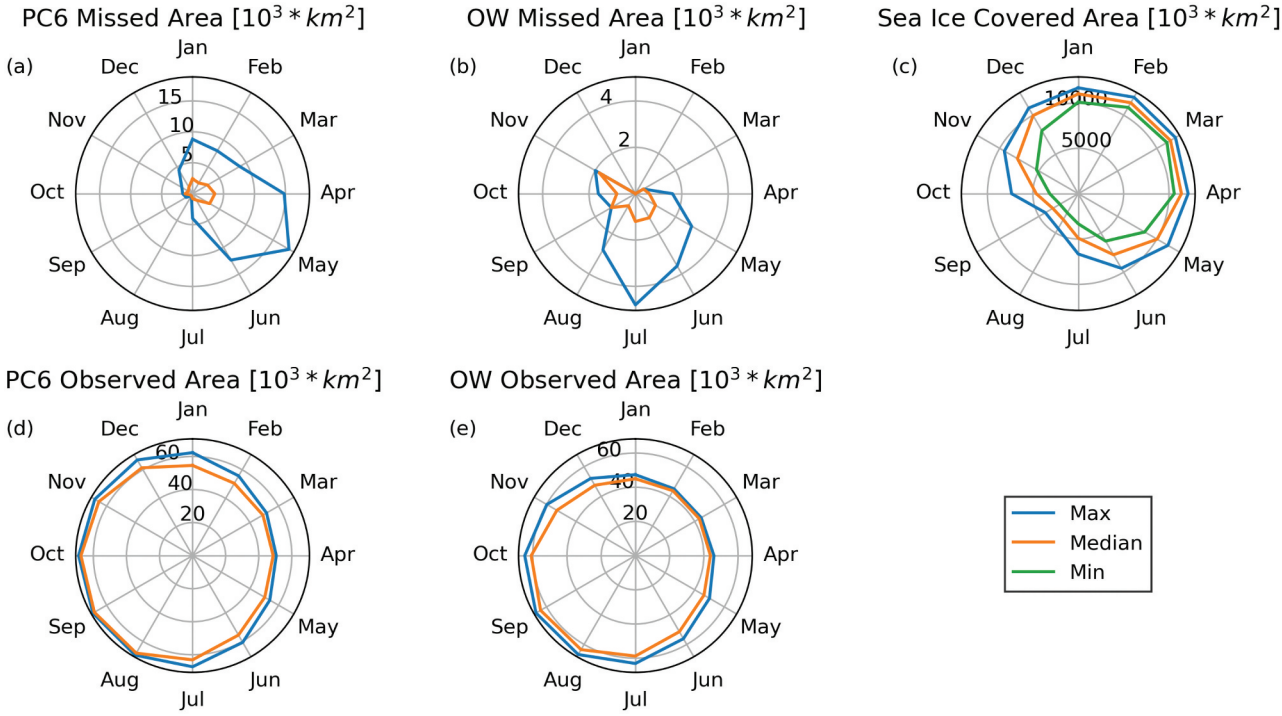

Figure 13. Metrics of the simulated Arctic accessibility maps from ATAM against observations from ASTD, calculated from 2013 to 2020. Missed area (a, b) indicates regions where ships have been observed but ATAM has falsely marked as inaccessible. Sea ice-covered area (c) is calculated for the Arctic region over 60° N. Observed area (d, e) indicates regions where a certain type of ships have been observed during the monthly period.

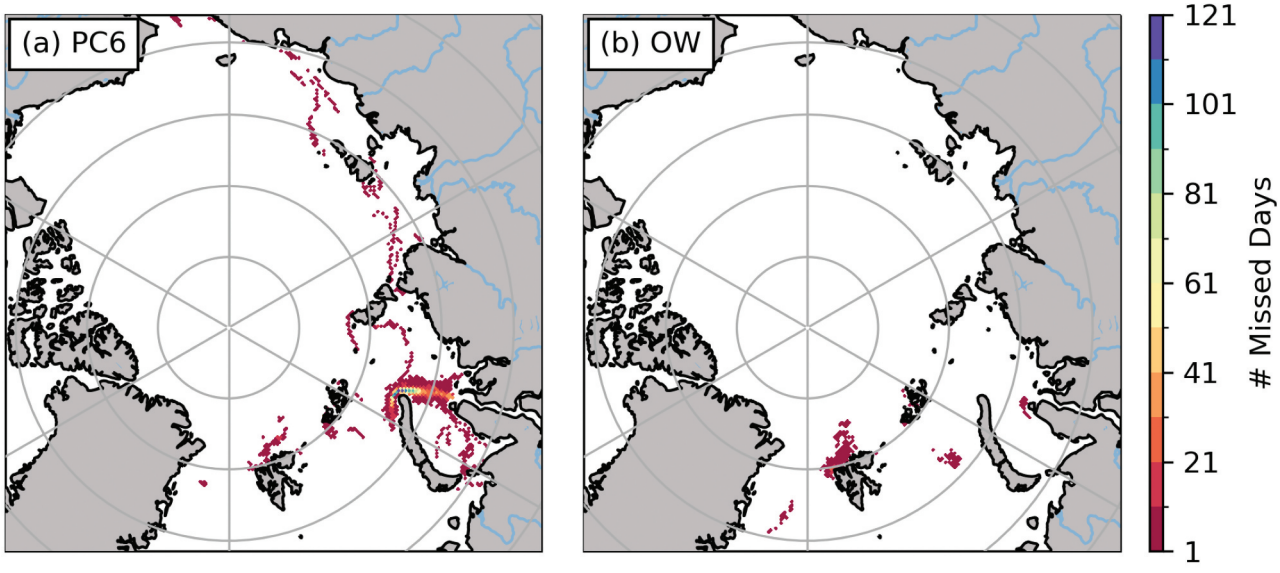

Figure 14. The total number of days from 2013 to 2020 when a grid is determined as inaccessible by ATAM but ships have been observed from ASTD.

into these areas to access rich fishing grounds and maximize their catch. Finally, passenger ships with thinner hulls or even without any ice strengthening can also have unexpected visits to regions with first-year ice or multi-year ice. Being scenic cruises, these cruises may include excursions into ice-infested areas to provide passengers with a close-up view of icebergs, glaciers and wildlife. Although not optimized for prolonged

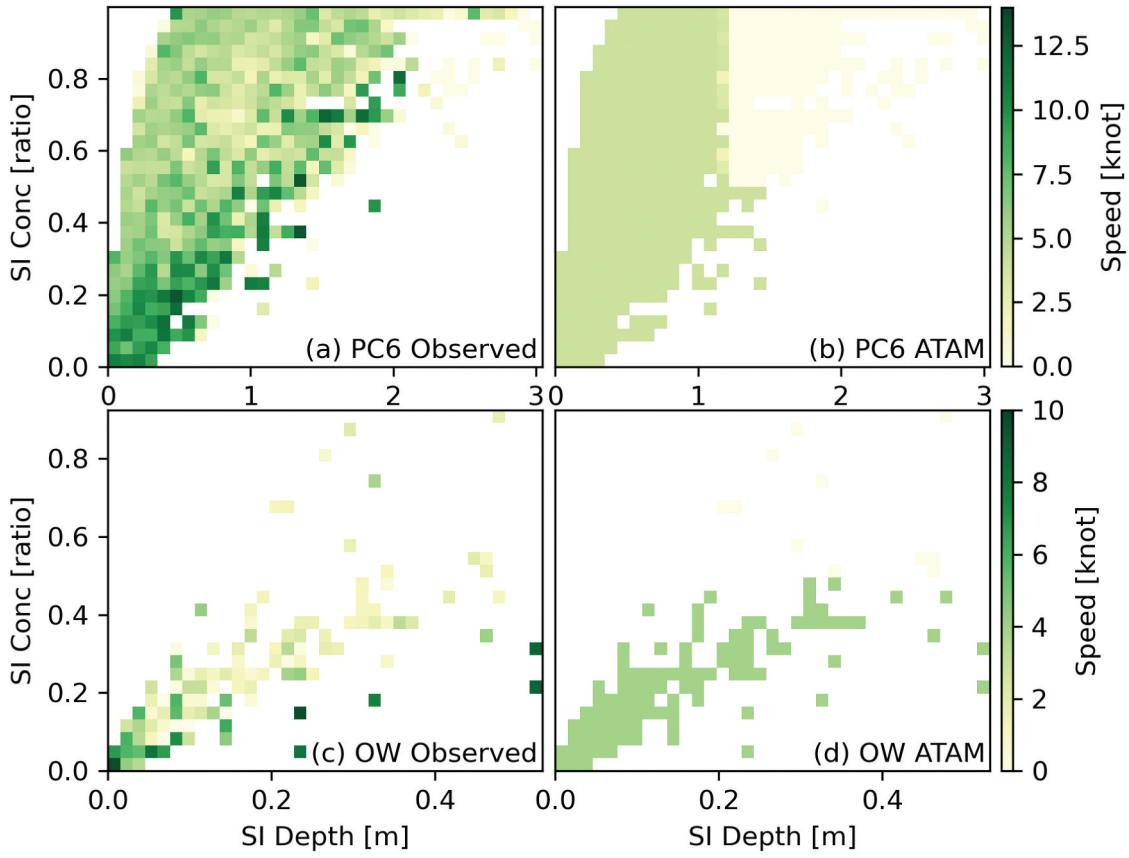

Figure 15. A comparison between the observed ship travel speed and the calculated speed from ATAM. The first row shows results for PC6 and the second row shows results for OW. The first column shows observed speed and the second column shows estimated speed from ATAM.

operation, they may still have safety features and procedures in place to mitigate risks associated with navigating including close monitoring of ice conditions and cooperation with icebreaker escorts.

In Figure 8 last column, FS II ships have been shown to access ice-infested regions. This could be possible when they are accompanied by additional ice breakers which are not reflected by this dataset. Another reason is due to PIOMAS model error since the sea ice depth is a simulated field, rather than observation. On the other hand, the FS 1A Super (first column) shows the highest capability in terms of sailing through ice, showing a large number of points, e.g. from cargo ships and tankers, from waters deeply covered in multi-year sea ice (sea ice depth larger than 1.5 metres).

5.4. Underestimation of arctic accessibility and travel speed

The validation of ATAM against observed ship data provides valuable insights into the model's performance and areas for improvement. The comparison highlights discrepancies in simulated accessibility, particularly in regions with complex ice conditions. The most important factor in the ATAM for determining accessibility is the calculation of ice numerals and the predefined ice multipliers. However, since the ice multipliers were simply parameterized, these coefficients could be out-of-date by current standards, which might be the biggest source of error.

In Figure 13, the largest error for PC6 was in May. This is because the Arctic undergoes a phase change around May from being inaccessible for PC6 ships to being accessible. The accessibility of winters and summers is relatively easy to model. However, uncertainty arises during the early stage of sea ice melting. In other words, the earliest time for PC6 to safely travel through the Arctic can range from April to June depending on the actual navigational conditions as well as the chosen route. The same observation can be made for OW but the maximum error happens in July. This is due to their different thicknesses in ice strengthening.

Furthermore, the spatial analysis of missed locations by ATAM reveals clustering around regions with

challenging ice conditions, indicating the model's tendency to be overly strict. This tendency highlights the importance of refining model parameters and incorporating real-time data to enhance accuracy. The underestimation of travel speed for ice-strengthened vessels and the lack of variability in speed estimation for ships without ice strengthening underscore the challenges in accurately modelling Arctic navigation dynamics.

6. Conclusion

This study analysed ship traffic patterns and accessibility modelling in the Arctic over an 8-year period from 2013 to 2020. By integrating reported ship tracking data from the ASTD with a sea ice reanalysis dataset, PIOMAS, we are able to map and assess spatiotemporal trends in Arctic shipping activity in relation to declining sea ice conditions. The comparison of simulated and observed ship traffic revealed important insights into the predictive capabilities of the ATAM.

The notable increase in maritime activities, particularly during the summer months, underscores the changing accessibility of Arctic waters driven by diminishing sea ice cover and improving navigational capabilities. Fishing vessels and cargo ships emerge as key contributors to this upward trajectory, reflecting both economic interests and the opening of new maritime routes.

Furthermore, the validation of the Arctic Traffic Accessibility Model (ATAM) against observed ship data reveals discrepancies in simulated accessibility, particularly in regions with complex ice conditions. The underestimation of travel speed for ice-strengthened vessels and the tendency of the model to be overly strict in certain regions underscore the challenges in accurately modelling Arctic navigation dynamics. In particular, the ATAM shows the highest error in the Kara Sea and the Barents Sea during spring and fall months. One limitation of the evaluation with only ASTD is the inevitable bias due to undersampling, meaning that observations are only available when there are ships. As a result, the navigable area defined by ASTD would be smaller than the actual accessible region.

We suggest future work to investigate model refinements that improve representations of ice conditions and navigability in the Kara Sea and the Barents Sea. Integrating higher-resolution ice concentration and thickness data focused on these regions may help address these issues as shipping activities are favouring these regions. But more importantly, a better parameterization scheme is needed to improve the quantification of accessibility. Current estimation is only conditioned on the sea ice but other factors can also influence routing decisions like ocean waves and wind. Further research can focus on enhancing model parameterization, for example, the derivation of the IN and the shipping speed, and integrating emerging and heterogeneous data sources to provide more accurate projections of Arctic marine access in a changing climate.

Broadly, more discussions are needed on the relationship between anthropogenic climate change and the increasing maritime accessibility in the Arctic. As global warming accelerates the melting of sea ice, it opens up new navigation routes, potentially boosting economic activities in the region. However, this accessibility comes with significant ethical and environmental challenges. The exploitation of these newly accessible areas must be balanced with sustainable practices to protect the fragile Arctic ecosystem. An in-depth examination of the ethical implications of increased Arctic traffic, including the impact on indigenous communities and wildlife, is crucial to ensure long-term environmental sustainability.

Disclosure statement

No potential conflict of interest was reported by the author(s).

Funding

This work was supported by grants from the Penn State Center for Security Research and Education (CSRE) and the Institute for Computational and Data Sciences (ICDS).

ORCID


Weiming Hu http://orcid.org/0000-0003-4501-1435

Data availability statement

The PIOMAS dataset can be openly accessed from https://psc.apl.uw.edu/research/projects/arctic-sea-ice-volume-anomaly/data/model_grid. The original dataset is unstructured. To accommodate our analysis workflow in Python, we developed a Python module to download, extract and re-grid the dataset into https://en.wikipedia.org/wiki/NetCDFNetCDF. Our open-source Python module can be found at https://github.com/Weiming-Hu/PyPIOMAS/.

The ASTD can be accessed from the official website, https://www.pame.is/index.php/projects/arctic-marine-shipping/astd#astd-access. If not a participating Arctic States or associated member, the user will need to pay a fee for access.

Other data used for analysis and visualization include the Arctic marine regions from https://www.marineregions.org/downloads.php#iho., the popular Arctic sea routes from https://arcg.is/0j1Wie., and the Arctic Ocean base map from https://arcg.is/0j1Ojq0.

References

Aksenov, Y., E. E. Popova, A. G. N. Andrew Yool, T. D. Williams, L. Bertino, J. Bergh, and J. Bergh. 2017. "On the Future Navigability of Arctic Sea Routes: High-Resolution Projections of the Arctic Ocean and Sea Ice." *Marine Policy* 75:0 300–317. https://doi.org/10.1016/j.marpol.2015.12.027.

Battistello, G., J. F. Gonzalez, M. Ulmke, W. Koch, and C. Mohrdieck. 2016. "Multi-Sensor Maritime Monitoring for the Canadian Arctic: Case Studies." *2016 19th International Conference on Information Fusion (FUSION)*, Heidelberg, Germany, 1881–1888.

Chen, Y., N. Lou, G. Liu, Y. Luan, and H. Jiang. 2022. "Risk Analysis of Ship Detention Defects Based on Association Rules." *Marine Policy* 142:0 105123. https://doi.org/10.1016/j.marpol.2022.105123.

Cohen, J., J. Screen, J. C. Furtado, M. Barlow, D. Whittleston, D. Coumou, J. Francis, et al. 2014. "Recent Arctic Amplification and Extreme Mid-Latitude Weather." *Nature Geoscience* 7:627–637. https://doi.org/10.1038/NGEO2234.

Crépin, A.-S., M. Karcher, and J.-C. Gascard. 2017. "Arctic Climate Change, Economy and Society (Access): Integrated Perspectives." *AMBIO: A Journal of the Human Environment* 46 (S3): 0 341–354. https://doi.org/10.1007/s13280-017-0953-3.

Dalsøren, S., B. Samset, G. Myhre, J. Corbett, R. Minjares, D. Lack, and J. Fuglestvedt. 2012. "Environmental Impacts of Shipping in 2030 with a Particular Focus on the Arctic Region." *Atmospheric Chemistry & Physics* 13 (4): 0 1941–1955. https://doi.org/10.5194/ACP-13-1941-2013.

Fiorini, M., A. Capata, and D. Bloisi. 2016. "Ais Data Visualization for Maritime Spatial Planning (Msp)." *International Journal of E-Navigation and Maritime Economy* 5:0 45–60. https://doi.org/10.1016/J.ENAVI.2016.12.004.

Garcia-Soto, C., L. Cheng, L. Caesar, S. Schmidtko, E. B. Jewett, A. Cheripka, I. Rigor et al. 2021. "An Overview of Ocean Climate Change Indicators: Sea Surface Temperature, Ocean Heat Content, Ocean Ph, Dissolved Oxygen Concentration, Arctic Sea Ice Extent, Thickness and Volume, Sea Level and Strength of the Amoc (Atlantic Meridional Overturning Circulation)." *Frontiers in Marine Science* 8:642372. https://doi.org/10.3389/fmars.2021.642372 .

Granier, C., U. Niemeier, J. Jungclaus, L. Emmons, P. Hess, J. Lamarque, S. Walters, and G. Brasseur. 2006. "Ozone Pollution from Future Ship Traffic in the Arctic Northern Passages." *Geophysical Research Letters* 33. https://doi.org/10.1029/2006GL026180.

Hendry, K. R., V. A. Huvenne, L. F. Robinson, A. Annett, M. Badger, A. W. Jacobel, H. Chin Ng, J. Opher, R. A. Pickering, M. L. Taylor, et al. 2019. "The Biogeochemical Impact of Glacial Meltwater from Southwest Greenland." *Progress in Oceanography* 176:102126. https://doi.org/10.1016/j.pocean.2019.102126.

Ho, J. 2010. "The Implications of Arctic Sea Ice Decline on Shipping." *Marine Policy* 34:0 713–715. https://doi.org/10.1016/J.MARPOL.2009.10.009.

Kwok, R., G. F. Cunningham, S. Kacimi, M. A. Webster, N. T. Kurtz, and A. A. Petty. 2020. "Decay of the Snow Cover Over Arctic Sea Ice from Icesat-2 Acquisitions During Summer Melt in 2019." *Geophysical Research Letters* 470 (12): 0 e2020GL088209. https://doi.org/10.1029/2020GL088209.

Lensu, M., and F. Goerlandt. 2019. "Big Maritime Data for the Baltic Sea with a Focus on the Winter Navigation System." *Marine Policy* 104:53–65. https://doi.org/10.1016/J.MARPOL.2019.02.038.

Marie, A. G., C. Comtois, and B. Slack. 2017. "Constraints on Canadian Arctic Maritime Connections." *Case Studies on Transport Policy* 5 (2): 0 355–366. https://doi.org/10.1016/J.CSTP.2017.03.004.

Martin, C. 1988. "William Scoresby, Jr. (1789-1857) and the Open Polar Sea - Myth and Reality." *Arctic* 41 (1): 0 39–47. https://doi.org/10.14430/ARCTIC1690.

Martin Bergström, B. L., and P. Kujala. 2020. *Future Scenarios for Arctic Shipping*. https://doi.org/10.1115/omae2020-18166.

McCallum, J. 1996. "Safe Speed in Ice: An Analysis of Transit Speed and Ice Decision Numerals." *Transport Canada*.

Meier, W. N., D. Perovich, S. Farrell, C. Haas, S. Hendricks, A. A. Petty, M. Webster et al. 2021. "Sea Ice." https://doi.org/10.25923/y2wd-fn85.

Melia, N., K. Haines, and E. Hawkins. 2016. "Sea Ice Decline and 21st Century Trans-Arctic Shipping Routes." *Geophysical Research Letters* 43 (18): 9720–9728. https://doi.org/10.1002/2016GL069315.

O'Rourke, R., 2023. Changes in the Arctic: Background and Issues for Congress. https://crsreports.congress.gov/product/pdf/R/R41153.

PAME. The Increase in Arctic Shipping 2013-2019: Arctic Shipping Status Report (Assr) #1. Technical Report, Protection of the Arctic Marine Environment (PAME). May 2020. URL. https://www.pame.is/projects/arctic-marine-shipping/arctic-shipping-status-reports.

Parkinson, C. L., and N. E. DiGirolamo. 2021. "Sea Ice Extents Continue to Set New Records: Arctic, Antarctic, and Global Results." *Remote Sensing of Environment* 267:0 112753. https://doi.org/10.1016/j.rse.2021.112753.

Pithan, F., and T. Mauritsen. 2014. "Arctic Amplification Dominated by Temperature Feedbacks in Contemporary Climate Models." *Nature Geoscience* 7:0 181–184. https://doi.org/10.1038/NGEO2071.

Saebi, M., J. Xu, S. R. Curasi, E. K. Grey, N. V. Chawla, and D. M. Lodge. 2020. "Network Analysis of Ballast-Mediated Species Transfer Reveals Important Introduction and Dispersal Patterns in the Arctic." *Scientific Reports* 100 (1): 0 19558. https://doi.org/10.1038/s41598-020-76602-4.

Saros, J. E., N. John Anderson, S. Juggins, S. McGowan, J. C. Yde, J. Telling, J. E. Bullard, M. L. Yallop, A. J. Heathcote, B. T. Burpee, et al. 2019. "Arctic Climate Shifts Drive Rapid Ecosystem Responses Across the West Greenland Landscape." *Environmental Research Letters* 140 (7): 074027. https://doi.org/10.1088/1748-9326/ab2928.

Schweiger, A., R. Lindsay, J. Zhang, M. Steele, H. Stern, and R. Kwok. 2011. "Uncertainty in Modeled Arctic Sea Ice Volume." *Journal of Geophysical Research: Oceans, 1160* C8. https://doi.org/10.1029/2011JC007084.

Screen, J. 2014. "Arctic Amplification Decreases Temperature Variance in Northern Mid- to High-Latitudes." *Nature Climate Change* 4:0 577–582. https://doi.org/10.1038/NCLIMATE2268.

Serreze, M., and J. Francis. 2006. "The Arctic Amplification Debate." *Climatic Change* 76:0 241–264. https://doi.org/10.1007/S10584-005-9017-Y.

Silber, G. K., and J. D. Adams. 2019. "Vessel Operations in the Arctic, 2015–2017." *Frontiers in Marine Science* 6:0 573. https://doi.org/10.3389/fmars.2019.00573.

Smith, L. C., and S. R. Stephenson. 2013. "New Trans-Arctic Shipping Routes Navigable by Midcentury." *Proceedings of the National Academy of Sciences* 110 (13): E1191–E1195. https://doi.org/10.1073/pnas.1214212110 .

Stephenson, S. R., L. C. Smith, and J. A. Agnew. 2011. "Divergent Long-Term Trajectories of Human Access to the Arctic." *Nature Climate Change* 10 (3): 0 156–160. https://doi.org/10.1038/nclimate1120.

Stephenson, S., and L. Smith. 2015. "Influence of Climate Model Variability on Projected Arctic Shipping Futures." *Earth's Future* 3. https://doi.org/10.1002/2015EF000317.

Stephenson, S., W. Wang, C. Zender, H. Wang, S. Davis, and P. Rasch. 2018. "Climatic Responses to Future Trans-Arctic Shipping." *Geophysical Research Letters* 45 (18): 9898–9908. https://doi.org/10.1029/2018GL078969.

Trusel, L. D., S. B. Das, M. B. Osman, M. J. Evans, B. E. Smith, X. Fettweis, J. R. McConnell, B. P. Noël, and M. R. van den Broeke. 2018. "Nonlinear Rise in Greenland Runoff in Response to Post-Industrial Arctic Warming." *Nature* 5640 (7734): 0 104–108. https://doi.org/10.1038/s41586-018-0752-4.

Turetsky, M. R., B. W. Abbott, M. C. Jones, K. Walter Anthony, D. Olefeldt, E. A. Schuur, G. Grosse, P. Kuhry, G. Hugelius, C. Koven, et al. 2020. "Carbon Release Through Abrupt Permafrost Thaw." *Nature Geoscience* 130 (2): 138–143. https://doi.org/10.1038/s41561-019-0526-0.

US Department of Defense. 2011. URL Report to Congress on Arctic Operations and the Northwest Passage. https://dod.defense.gov/Portals/1/Documents/pubs/Tab_A_Arctic_Report_Public.pdf.

Wang, X., J. Key, R. Kwok, and J. Zhang. 2016. "Comparison of Arctic Sea Ice Thickness from Satellites, Aircraft, and Piomas Data." *Remote Sensing* 80 (9): 0 713. https://doi.org/10.3390/rs8090713.

White House. 2022. URL National Strategy for the Arctic Region." https://www.whitehouse.gov/wp-content/uploads/2022/10/National-Strategy-for-the-Arctic-Region.pdf.

Xiao, F., H. Ligteringen, C. Gulijk, and B. Ale. 2015. "Comparison Study on Ais Data of Ship Traffic Behavior." *Ocean Engineering* 95:0 84–93. https://doi.org/10.1016/J.OCEANENG.2014.11.020.

Zhang, J., and D. Andrew Rothrock. 2003. "Modeling Global Sea Ice with a Thickness and Enthalpy Distribution Model in Generalized Curvilinear Coordinates." *Monthly Weather Review, 50* 131 (5): 0 845–861. https://doi.org/10.1175/1520-0493(2003)131<0845:MGSIWA>2.0.CO;2.